Sensors and Actuators B 218 (2015) 237–244

Contents lists available at ScienceDirect

Sensors and Actuators B: Chemical

journal homepage: www.elsevier.com/locate/snb

A novel revolving piston minipump

Majid Ashouri, Mohammad Behshad Shafii*, Ali Moosavi, Hamid Amiri Hezave

School of Mechanical Engineering, Sharif University of Technology, Tehran, Iran

ARTICLE INFO

Article history:
Received 14 February 2015
Received in revised form 23 April 2015
Accepted 27 April 2015
Available online 6 May 2015

Keywords:
Ferrofluid
Magnetic actuator
Micropump
PMMA channel
Revolving piston

ABSTRACT

In this study, a novel prototype high-efficiency miniature pump that uses magnetic properties of a ferrofluid in both pumping and valving mechanisms is presented. The minichannel consisting of a cylindrical pumping chamber, a check valve, an inlet and an outlet, comprises six bonded layers of PMMA. A cylindrical permanent magnet that is placed inside the chamber and is externally actuated by a motorized off-center permanent magnet, functions as a revolving piston which sweeps the perimeter of the cylinder. Ferrofluid is used to cover the gaps between the magnetic piston and the channel walls, also serves as a separating plug between the inlet and the outlet of the chamber preventing recirculation of the pumped fluid inside the chamber. This novel revolving piston design eliminates the need for an inlet valve. Pressure head is maintained using one ball check valve at the outlet of the pump. Water has been successfully pumped at flow rates of up to 934 μL/min, backpressures of up to 994 Pa, and maximum achieved volumetric efficiency of 79 percent while working at 80, 52, and 9 rpm rates, respectively.

1. Introduction

With a growing interest in the development of microfluidic systems over the past two decades, there have been numerous reports on the fabrication of microfluidic devices for use in a wide range of applications, such as chemical analysis, biological and chemical sensing, drug delivery, molecular separation such as DNA analysis, amplification, sequencing or synthesis of nucleic acids, environmental monitoring, and also in precision control systems for automotive, aerospace and machine tool industries. Several micropumps have been developed for the purpose of microscale pumping of fluidic samples. Various pumping principles with different actuation mechanisms have been investigated including electrostatic, piezoelectric, thermal, pneumatic, shape memory alloy, bimetallic, ion conductive polymer film, electromagnetic, magnetic, phase change, magnetohydrodynamic, electrohydrodynamic, electroosmotic, electrowetting, bubble type, flexural planar wave, electrochemical, and evaporation based; reviewed in [1–4].

Micropumps made of polymeric materials with contactless external actuations are of particular interest for disposable applications with the reusability of the costly parts of the device. In particular, magnetic actuation has the advantages of rapid time response with low actuation voltage as well as large displacement with the ability of self-priming. Several magnetically driven micropumps were presented based on deflection of elastic membranes with embedded permanent magnet using external electromagnets [5–9] or external permanent magnets with controllable movement [9–11]. The former actuation method has an issue of heating whereas the latter one has the advantage of lower input power.

On the other hand, most of the investigated pumping and valving devices are relatively complex and need expensive precision micromachining technologies. Among the microfabricated systems, ferrofluidic devices have the advantage of obviating the required tolerance of the micromachined channels or the allowances needed for the microfabricated moving parts; thereby reducing the cost as well as improving the reliability; because ferrofluids (colloidal liquid made of nanosize ferromagnetic particles suspended in a carrier fluid) have the benefit of conforming to different channel shapes and providing self-sealing capability with low friction in motion responding to imposed magnetic fields. The use of magnetism for controlling fluidic functions such as pumping, mixing, magnetowetting, and magnetic manipulation of particles are reviewed in [12]. A review of the recent advances in mechanical applications of ferrofluids is provided by Torres-Díaz and Rinaldi [13].

Many researchers used the self-sealing property of ferrofluid plugs actuated by permanent magnets or electromagnetic coils for pumping and valving functions in microchannels. The ferrofluidic micropumps usually withstand the low pressure in the order of 1 kPa which can be increased with decreasing the dimensions of

* Corresponding author at: P.O. Box 11365-9567, Tehran, Iran. Tel.: +98 21 66165675; fax: +98 21 66000021.
E-mail address: behshad@sharif.edu (M.B. Shafii).

http://dx.doi.org/10.1016/j.snb.2015.04.104
0925-4005/

the microchannel or increasing the strength of the applied magnetic field. With the advantages of low complexity and low cost while reducing total pump volume, for example, these pumps can be employed to circulate the cooling liquid through micro heat exchangers [4]. Wagner et al. [14] demonstrated the displacement of ferrofluids activated by the linear movement of an external motorized permanent magnet inside a minichannel. Greivell and Hannaford [15] proposed an electromagnetic micropipette using a ferrofluid. Pérez-Castillejos et al. [16] reported the capability of the use of ferrofluids in microactuators due to pressure generation in the presence of magnetic field. Hatch et al. [17] designed a ferrofluidic micropump using rotating motion of ferrofluid in a ring channel where magnetically actuated plugs of ferrofluid served both for pumping and valving. Based on the foresaid idea, Kim et al. [18] proposed a peristaltic micropump using magnetic fluid without any contamination of the working fluid. In Ref. [19], an actuation mechanism similar to that of a stepper motor has been used to demonstrate a circular micropump with a ferrofluid plug as the rotor or the driving piston and eight solenoids as the stator. The authors stated that the developed stepper micropump with the capability of precise positioning of the ferrofluid plug would allow a more flexible polymerase chain reaction (PCR) protocol and can work with the ferrofluid driven microchip for rapid PCR reported previously by their group [20]. Yamahata et al. [21] used a ferrofluidic plug as a piston in a micropump with two check valves. Hartshorne et al. [22] demonstrated the use of ferrofluid in two types of microvalves as Y-valve and well-valve and also presented a ferrofluidic piston micropump with a ferrofluid plug as a piston and two ferrofluidic "well" valves controlled by the movements of external permanent magnets. Ando et al. [23] introduced a pump that consisted of a single volume of ferrofluid held flattened at the bottom of a pipe by a fixed permanent magnet. An array of five electromagnets allowed for the formation and the movement of a ferrofluidic cap acting simultaneously like a valve and a plunger. They also controlled and synchronized the actuation of three ferrofluid plugs in a tube using external electromagnets to pump an immiscible fluid [24].

In this study, design, fabrication and characterization of a novel magnetically actuated miniature pump is presented. It consists of a polymethyl methacrylate (PMMA) casing of circular cross-section, a revolving disk inside it, and a check valve at the outlet. The pumping is based on the peripheral displacement of the disk piston inside the cylindrical chamber. The disk is a permanent magnet which is externally actuated using another cylindrical permanent magnet driven by a motor. Ferrofluid is employed to maintain sealing by filling the gaps between the magnetic disk and the chamber walls. Also, a combination of ferrofluid and an external stationary permanent magnet is used to form a physical barrier between the inlet and the outlet ports. Continuous high performance pumping, working at relatively low voltages, simple design, easy fabrication, and low cost manufacturing are the main advantages of this miniature pump. With the avail of non-contact external actuation, this pump can be used in many applications when microfluidic systems need to be disposable and low cost.

2. Working principle

The pumping mechanism is based on the peripheral sliding motion of a disk inside a cylinder. A schematic of the pump is given in Fig. 1a. The pump consists of a cylindrical chamber with one inlet port and one outlet port, one passive valve at the outlet, and a revolving disk piston inside the chamber. The disk piston is a permanent magnet which is externally actuated using another cylindrical permanent magnet driven by a motor. The rotating shaft of the motor has its axis of rotation that matches with the centerline of the chamber; however, it is eccentric with respect to the revolving piston. The magnetic piston is fully covered with ferrofluid which is held to the surface of the disk by its magnetic force. The ferrofluid fills the gaps between the cylindrical magnet and the chamber walls to maintain sealing. Serving as the sliding vane in a "roller compressor", a narrow plug of ferrofluid which is held by an external stationary permanent magnet is always present in the upper section of the chamber between the inlet and the outlet ports.

As demonstrated in Fig. 1, the pump does not require an inlet valve but requires an outlet valve. The sealing between the high and low pressure sides has to be provided along the line of contact between the piston and the cylinder block, that is along a line staring from the small sector between the inlet and the outlet ports to the piston as well as the piston and the end pates of the chamber. The effectiveness of the ferrofluidic sealing depends mainly on the strength of the magnetic fields and the piston speed and partly on the clearance, surface finish and ferrofluid viscosity.

As long as the force imposed by the pressure gradient does not exceed the force generated by the external stationary permanent magnet, the ferrofluid will block the section between the inlet and the outlet ports. On the other hand, the rpm of the motor rotating the external actuator of the revolving piston should be low enough to impose the required force to the piston to follow the path of the moving external magnetic field.

The ferrofluid is always exposed to the magnetic fields of all the magnets. Therefore, as illustrated in Fig. 1, a contiguous ferrofluidic plug will be established between the piston and the stationary magnet in the chamber as it revolves. When the magnetic piston moves away from the region around the stationary magnet, a portion of the ferrofluid is more strongly affected by the field of the magnetic piston and sticks to its surface. Therefore, a plug of ferrofluid goes along with the translating magnetic piston while another plug is always held in the small sector below the stationary permanent magnet. The dimensions of the system and the employed magnetic fields should be compatible as to never let the two plugs of ferrofluid separate from each other as well as staying as thick as the height of the chamber.

The functional principle of the pump is schematically described in Fig. 1. In this figure, there are two distinct situations for the pumping phases based on the location of the revolving piston: the case when the revolving piston is sweeping the larger sector between the inlet and the outlet ports (Fig. 1a–c) and the case when it is confined to the small sector between the inlet and the outlet ports (Fig. 1d). In the first case, the revolving piston sweeps the chamber counterclockwise from the inlet to the outlet as shown in Fig. 1a–c. As the result, the displaced volume of the working fluid will be pushed into the outlet port. In the second case, as it is shown in Fig. 1d, by approaching the revolving piston to the region between the inlet and the outlet of the chamber, they become accessible to each other through the part of the chamber at opposite side of the stationary permanent magnet. In this situation, the check valve located after the outlet will resist the fluid from flowing reversely from the outlet port to the inlet port. So, during the second situation, there is no significant reverse flow of fluid through the pump. Therefore, in a complete cycle, a net positive fluid flow from the inlet into the outlet will be established which is in the order of the volume of the chamber excluding the spaces occupied by the piston and the ferrofluid.

The geometry of the piston movement inside the cylinder is shown in Fig. 2. The instantaneous volumetric flow rate of the pump can be roughly estimated by the differential sweeping volume of the piston. This can be expressed by the rate of change in the shaded area in Fig. 2 which is approximately given by Eq. (1). Also, an estimation of the theoretical average volumetric flow rate of working fluid through the pump which is expressed by the free volume inside the cylinder is given by Eq. (2).

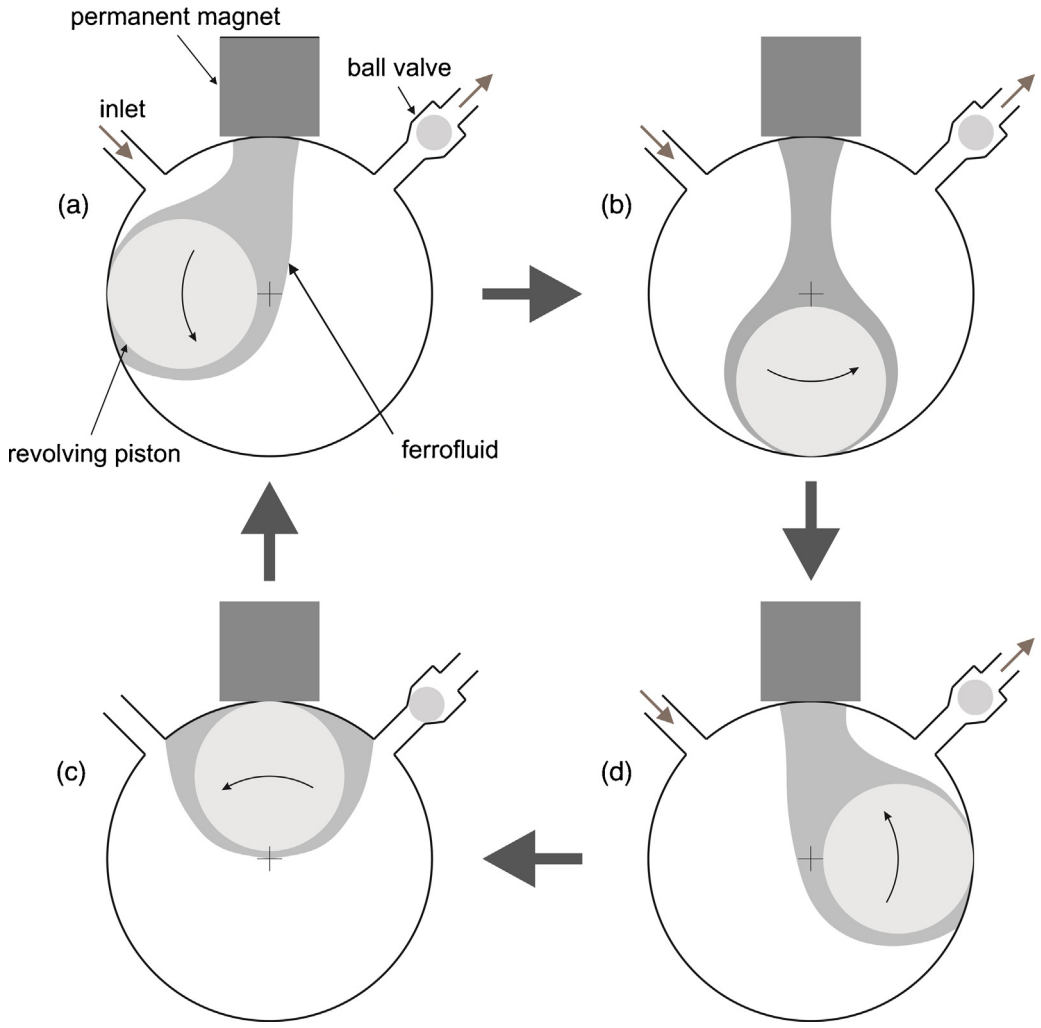

Fig. 1. Schematic of the working principle of the pump; the revolving piston sweeps the fluid inside the chamber from the inlet to the outlet in parts (a), (b), and (c). In part (d), the revolving piston has reached the region between the inlet and the outlet ports. In this condition, there is no net flow while the valve is closed, preventing reverse flow.

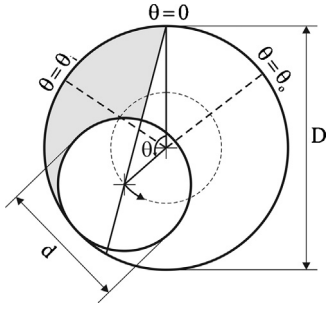

Fig. 2. Illustration of the pumping geometry.

$$q(\theta) = \pi N D^2 H \frac{1 - \frac{d}{D} - \cos(\theta)}{1 - \frac{d}{D} + \frac{1}{1-\frac{d}{D}} - 2\cos(\theta)} \quad (1)$$

$$Q = N\left[\frac{\pi}{4}(D^2H - d^2h) - V_f\right] \quad (2)$$

In Eqs. (1) and (2), $q(\theta)$ and Q are in μL/min; D is the inner diameter of the cylinder (mm), d is the diameter of the piston (mm), H is the height of the cylinder block (mm), h is the height of the piston (mm), V_f is the volume of the injected ferrofluid (μL), and N is the rotational speed of the revolving piston (RPM).

In Eq. (1), it is obvious that integrating the flow rate over a complete cycle results in zero value. Actually, the inlet and outlet of the pump were not considered in the closed volume of Fig. 2. Therefore, Eq. (1) can only be used for θ values after the inlet port and before the outlet port (specified by θ_i and θ_o, respectively in Fig. 2). On the other hand, the presence of ferrofluid either between the inlet and outlet or around the piston were not included in Eq. (1). It is noted that, the efficiencies of either the ferrofluid or the check valve were not considered in Eqs. (1) and (2).

3. Structure and fabrication

According to the exploded view of the pump body, shown in Fig. 3a, the designed pump was composed of six joined PMMA 1 mm thick plates. The CO_2 laser based cutting method was used as a fast prototyping and low cost CNC microfabrication technique. The hot press machine was used for pressurized thermal bonding of PMMA plates. In order to enhance the quality of the bonding, chloroform as a chemical solvent was sprayed on the surfaces of the plates to be pressed.

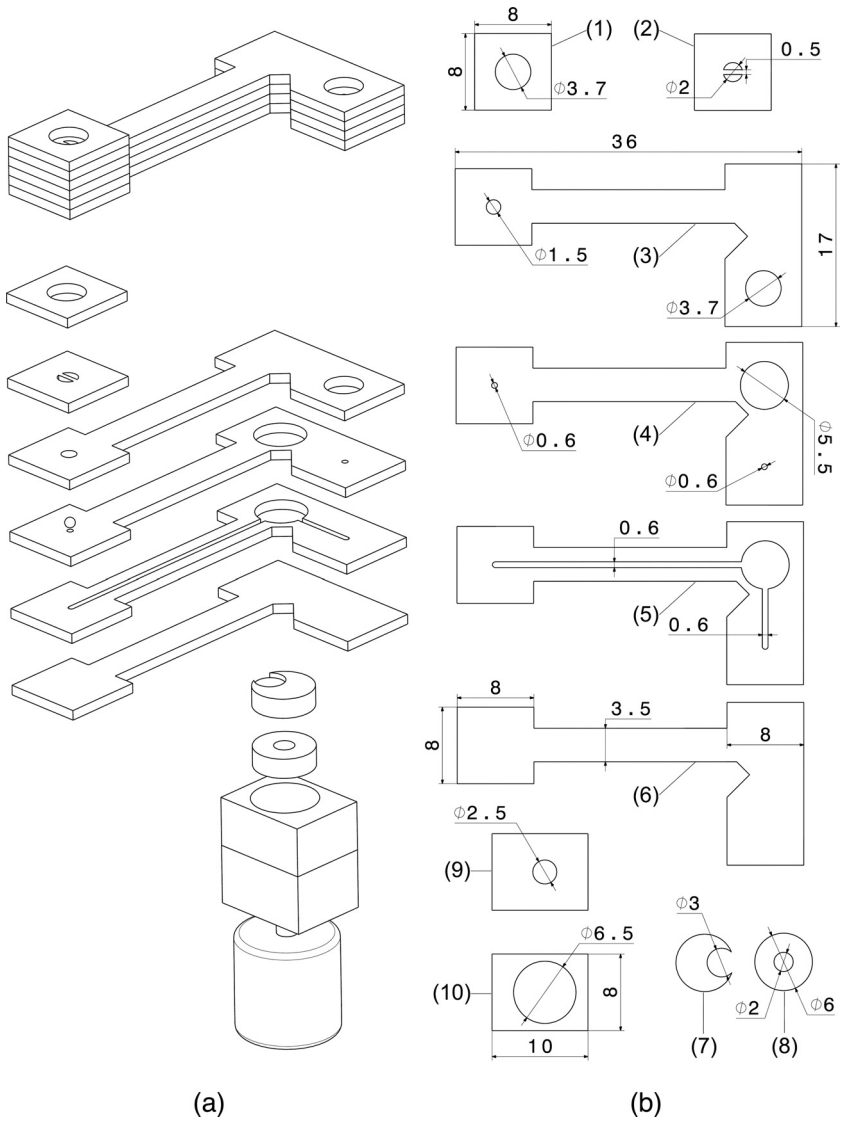

Fig. 3. Presentation of the design specifications of the minipump; (a) the assembled body and the exploded view, and (b) the characteristic dimensions of the pump elements.

The main geometrical parameters of the pump channel are shown in Fig. 3b. The numbers assigned to the parts refer to their placement from topside in the exploded view of Fig. 3a. A cylindrical permanent magnet having a surface magnetic field strength of 0.4 T with dimensions of 3 mm × 1.5 mm (diameter × height) was used inside the cylinder as the actuation piston. The ball valve consisted of a 1 mm in diameter stainless steel sphere inside a cylindrical chamber (part 3), which was connected to a circular seat (part 4) from bottom and a stopper (part 2) from top. The valve was normally closed; the ball moved upward under negative pressure. A 20 mm in length channel was considered between the valve chamber and the outlet of the pump keeping the ball insusceptible to the magnetic fields.

A cylindrical permanent magnet with both diameter and height of 3 mm having a surface magnetic field strength of 0.51 T was employed to induce the actuation force to the magnetic piston. The magnet was placed in part 7 (Fig. 3b), then mounted on the axis of a 6 V DC gear motor. The center of the magnet was set at a diameter of 3.5 mm (0.5 mm more off-center than the dictated radius by the path of the piston shown in Fig. 2) to make the magnet tight to the perimeter of the chamber. For the ferrofluidic separating plug between the inlet and the outlet of the pumping chamber, the external magnetic field was provided by a set of cylindrical permanent magnets with 3 mm in diameter and total of 4.5 mm in height (total surface magnetic field strength of 0.54 T). Both external permanent magnets were located at the surface of the pump body. It is noted that, all the permanent magnets were axially magnetized NdFeB grade 35 with residual induction of 1.2 T (Shenzhen Shan Magnetism Industry Co., China). Fig. 4 shows the complete fabricated minipump together with the external actuators. Two graduated cylinders were mounted on the inlet and outlet ports of the pump for measuring the flow rate and backpressure.

After assembling the pump body, 20 μL of ferrofluid was injected through the hole on the upper plate using a needle. The amount of the injected ferrofluid was such that it formed a contiguous plug and maintained the required sealing. The ferrofluid must be immiscible with the fluid being pumped in order to be fully retained inside the channel during operation of the device. An oil based ferrofluid was utilized in the pump. The ferrofluid 'EFH1' was purchased from Ferrotec, USA. This ferrofluid uses a light hydrocarbon mineral oil as carrier liquid, which could be considered as immiscible with water (the working fluid in the tests). It contains magnetic nanoparticles with nominal diameter of 10 nm with a concentration of 7.9% by volume. The saturation magnetization and the initial susceptibility of this ferrofluid are 44 mT and 2.64, respectively [25].

Fig. 4. The complete minipump including the external actuator.

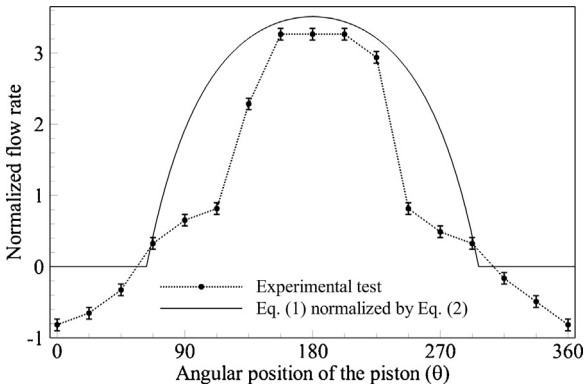

Fig. 5. Variations of flow rate during a complete pumping cycle at the operating rate of 9 rpm.

4. Characterization

To characterize the pump, water was used as the working fluid. Pressure heads and flow rates were measured by reading the difference in water levels and determining the rate of changes in water volume (in the specified time intervals), respectively, in the two vertical graduated cylinders installed on the inlet and outlet of the pump. The water surface was traced in differential time intervals to obtain the flow rate and backpressure. The images extracted from the captured video of the cylinders using a high resolution CCD camera were processed to characterize the pump performance. For the accuracy assessment, every experimental test was repeated five times and the mean values were reported, unless otherwise noted. Motor speed was observed to vary less than 1.5% throughout the repeated experiments. Before conducting the experiments, the newly assembled pump was left running at zero backpressure for few minutes.

Fig. 5 shows the variations of the normalized instantaneous flow rate (normal to the average flow rate) during a complete pumping cycle with minimal backpressure at the rate of 9 rpm. Different stages of this pumping loop are shown in Fig. 6 which presents the snapshots of the counterclockwise rotation of the piston at positions (a) $\theta = 0$, (b) $\theta = 5\pi/16$, (c) $\theta = \pi$, and (d) $\theta = 41\pi/24$. The case when the revolving piston was adjacent to the center of small sector between the inlet and the outlet ports is assigned to the position $\theta = 0$ and so on (Fig. 2). At the end of the cycle, a net average flow rate of 120 μL/min was resulted from the average positive flow rate of 137 μL/min (about 15 μL per revolution) for $5\pi/16 < \theta < 41\pi/24$ and the average negative reversal flow rate of 17 μL/min (about 2 μL per revolution) for other θ positions of the piston. In order to measure the instantaneous flow rate, the recorded video of the glass cylinder at the outlet was processed to obtain the differential movements of the water surface in the glass cylinder. In Fig. 5, the error bars show the uncertainties in the once conducted measurements associated with the 1 pixel probable error of reading the water levels in the two corresponding images of every data. It is noted that, the condition of minimal backpressure was true throughout the measurement with a maximum pressure difference of 7 Pa.

The theoretical instantaneous volumetric flow rate of the pump predicted by Eq. (1) which was normalized by the theoretical overall volumetric flow rate given by Eq. (2) is also presented in Fig. 5. To sketch this curve, the check valve of the pump was assumed to work ideally; hence, whenever the negative flow rate was obtained using Eq. (1), its value was considered to be zero. The maximum instantaneous flow rate was observed around $\theta = \pi$ where the piston had the highest differential sweeping volume. The difference between the experimental and theoretical data was due to the simplifications and approximations related to Eqs. (1) and (2). The ferrofluid added to the pumping chamber was not included in Eq. (1) where in addition to the resulted dead volume, the transformative shape of the ferrofluid plug and the probable inefficiency in its sealing to the flow passage through the complete cycle affects the real condition performance. Furthermore, the check valve located at the outlet of the pump was not ideal; hence, a reversal flow was observed in the experiment.

The flow rate-backpressure characteristics of the pump are shown in Fig. 7 for three different actuation rates of 23, 52, and 80 rpm. The maximum backpressures of 976, 994, and 924 Pa were achieved at operating rates of 23, 52, and 80 rpm, respectively. It can be deduced that, at higher speeds (e.g. 80 rpm), the maximum backpressure decreases due to limitations related to the sealing properties of the check valve and the ferrofluid.

Fig. 8 shows the measured flow rate at zero backpressure and the corresponding volumetric efficiency versus the actuation rate. The total theoretical displaced volume of the working fluid in one pumping cycle was approximately 17 microliter per revolution. As expected, initially the flow rate increased linearly with rpm; then at higher speeds, its rate dropped that is to say the volumetric efficiency decreased. The volumetric efficiency decreased with rpm due to inefficiency of the ferrofluid. On the other hand, at very high speeds, the piston was unable to properly follow the movement of the external magnetic actuator. Therefore, it can be deduced that by increasing the rpm, the volumetric efficiency constantly decreases and the flow rate reaches its maximum value followed by sharp decrease (not shown here). At the speed of 9 rpm with the highest efficiency of 79%, the piston translated with the velocity of 1.18 mm/s; the slow movement of the piston has assured the proper functionality of the sealing property of the ferrofluid.

The useful power and the consumed power are important characteristic parameters. Fig. 9 presents the useful power of the pump against the backpressure for three different actuation rates of 23, 52, and 80 rpm. The useful power has been evaluated by recasting the data provided in Fig. 7 as the flow rate-backpressure product. This is evident that the useful power is zero when the fluid is pumped under no backpressure as well as when the pump is

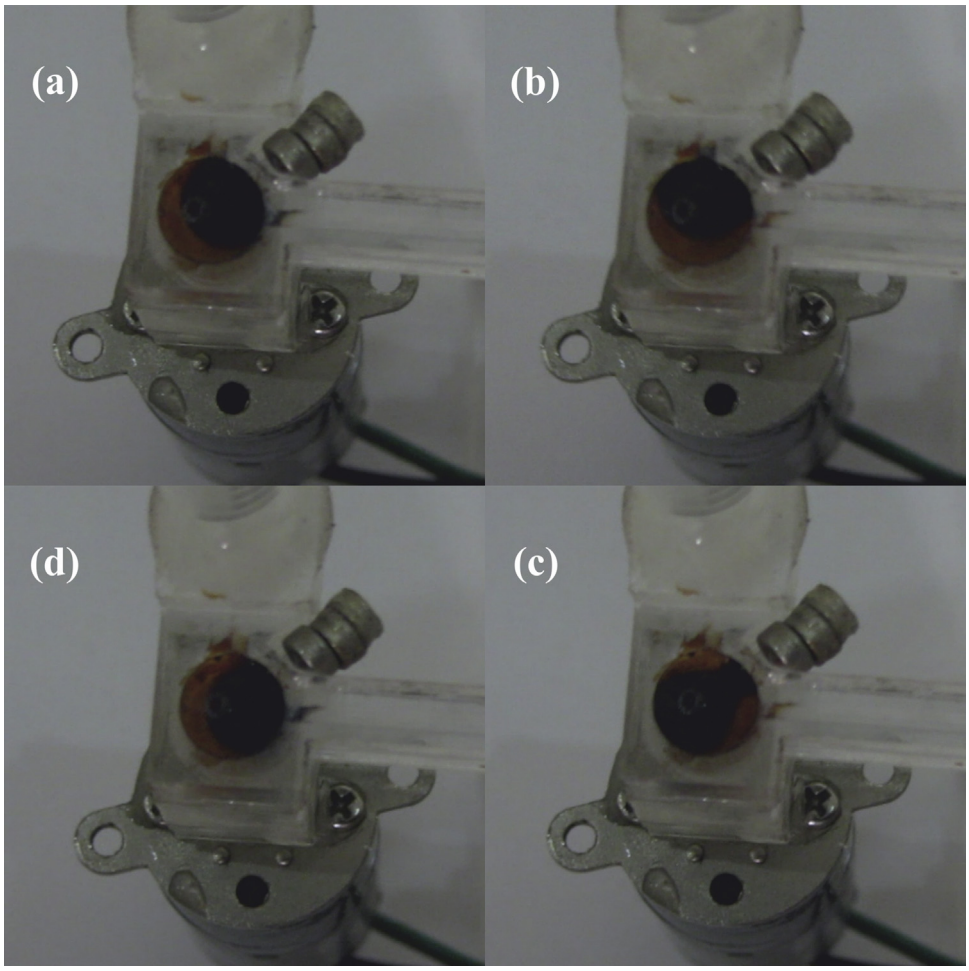

Fig. 6. Snapshots of pumping loop of the device. In part (a) with $\theta = 0$, the revolving piston was adjacent to the region between the inlet and the outlet ports. From part (b) with $\theta = 5\pi/16$ to part (d) with $\theta = 41\pi/24$, the counterclockwise rotation of the piston swept the fluid inside the chamber from the inlet to the outlet; its maximum rate occurred around part (c) with $\theta = \pi$.

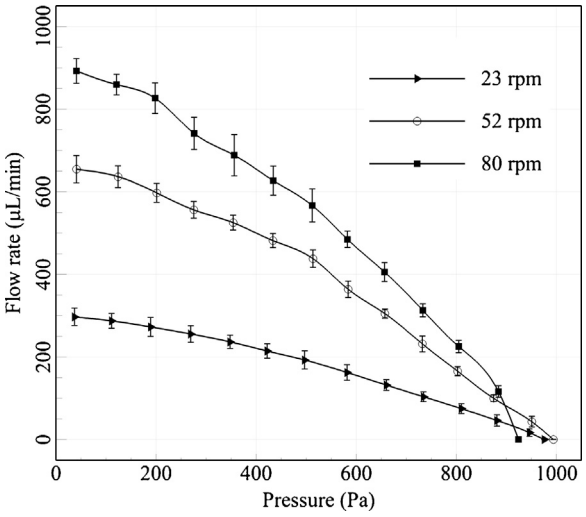

Fig. 7. The characteristic curve of the pump for different actuation rates.

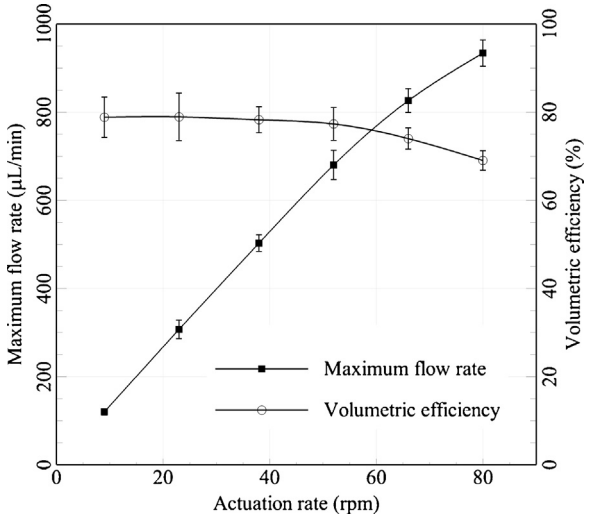

Fig. 8. The maximum flow rate and volumetric efficiency versus actuation rate.

operating at maximum achievable backpressure (i.e., zero flow rate). The maximum value of the useful power (the pumped energy) occurred at an intermediate value of backpressure. The data associated with the power are gathered in Table 1 for the aforementioned actuation rates. Operating at speeds of 23, 52, and 80 rpm, the applied voltages were 2, 4, and 6 V, respectively. The best thermodynamic efficiency (the useful power over total power consumption) was observed at 52 rpm (which had the best pressure head and a high volumetric efficiency, i.e. 77%) while pumping with the rate of 438 μL/min at a backpressure of 514 Pa.

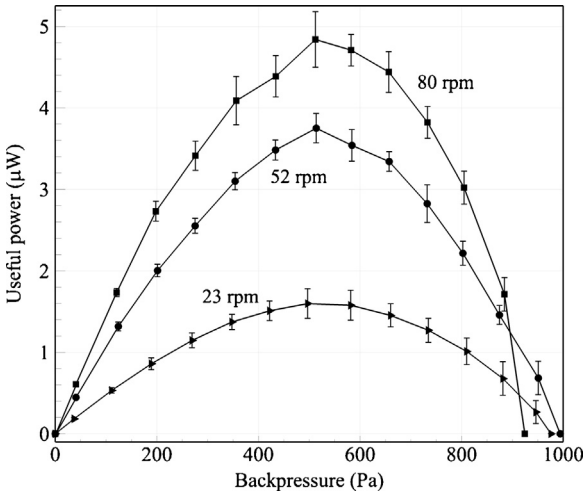

Fig. 9. Variations of the useful power against the backpressure for different actuation rates.

Table 1
Power data for different actuation rates.

	23 rpm	52 rpm	80 rpm
Maximum useful power (μW)	1.60 ± 0.18	3.75 ± 0.18	4.84 ± 0.34
Consumed power (mW)	60 ± 5	140 ± 7.5	240 ± 10
Maximum thermodynamic efficiency (10^{-3}%)	2.66 ± 0.52	2.68 ± 0.27	2.02 ± 0.23

Table 2
Performance comparison of the present pump with the reported ferrofluidic micropumps.

Actuation rate (rpm)	Ref. [17]	Ref. [21]	Present pump		
	8	5	23	52	80
Maximum head (Pa)	1320	2500	976	994	924
Flow rate[a] (μL/min)	46/38	31/26	307/191	680/445	934/576
Volumetric efficiency[a] (%)	73/60	62/52	79/49	77/50	69/42
Pumped energy per cycle (μJ)	0.46	3.61	4.17	4.33	3.63
Self-pumping frequency[b] (min^{-1})	0.113[c]	0.006	0.256	0.567	0.778

[a] In each column, the first data presents the evaluated parameter at zero backpressure while the second data reports its value at a backpressure of 500 Pa.
[b] The volumes of external actuators were not included.
[c] Based on an estimated overall volume.

As the last discussion, the performance of this novel pump was compared to some previously reported ferrofluidic micropumps as listed in Table 2. The comparisons were based on the maximum backpressure, pumped energy per cycle, self-pumping frequency, maximum flow rate, maximum volumetric efficiency, and flow rate and volumetric efficiency at a backpressure of 500 Pa. The pumped energy per cycle [1] was defined as the maximum value of the useful power obtained in a single pumping cycle. The self-pumping frequency was defined as the ratio of maximum flow rate to the package size [3]. The overall size of the pump body was about 1.2 cm^3. The presence of an external actuator incapacitated the miniaturization by 5.6 cm^3 extension in the overall size. Thus, the maximum recorded pumping flow rate at zero backpressure of 934 μL/min (at 80 rpm), gave a self-pumping frequency of 0.137 min^{-1}. However, the reported values of self-pumping frequency in Table 2 are based on the overall sizes excluding external actuators. As can be seen in Table 2, the present device had the best self-pumping frequency and the highest volumetric efficiency as well as the pumped energy per cycle. The inferiority in the maximum pressure head could be enhanced by improving the check valve, also applying an appropriate set of magnetic fields to a proper sizing of the device.

5. Conclusion

A novel prototype magnetically actuated piston minipump was presented. The pump was made of PMMA and consisted of a cylindrical chamber with one inlet port and one outlet port. The main components of the pump were (1) a ball check valve at the outlet, (2) a non-reciprocating revolving disk piston inside the chamber, (3) an external electric motor driving a permanent magnet for the actuation of the piston, (4) an external stationary permanent magnet for the valving function, and (5) some oil based ferrofluid inside the chamber functioning as the sealant between the piston and the cylinder walls as well as the valving between the inlet and the outlet. The combination of ferrofluid with permanent magnet inside the channel had the advantage of an auto-sealing ferrofluidic plug in the channel with low degradation of the ferrofluid over time. Thus, the device did not require precision microfabrication with small-clearance moving piston. In summary, the use of ferrofluid in the presented design provides ease of manufacture even if fabricated in smaller scales, easy and uncomplicated actuation, and the capability of the pump body to be disposable in light expense due to the external actuation.

The experimental tests were performed to characterize the flow rate–backpressure performance of the prototype pump at different actuation rates. In summary, some points were found:

- The magnetic actuation allowed low voltages and low power-consumption operations of the pump. At full speed rotation of the actuator, voltage and power of 6 V and 240 mW were needed, respectively.
- At low rpm, the flow rate increased linearly with the actuation rate while at higher speeds, its rate as well as the volumetric efficiency dropped due to inefficiency of the sealing capability of the ferrofluid. Hence, the device would be more functional if lower actuation rates, i.e. lower piston speeds, were applied. At best, about 12% of the volume of the fluid pumped to the outlet went back to the chamber giving a maximum volumetric efficiency of 79%.
- The conducted experiments showed that the pump was capable of reaching a flow rate of 934 μL/min and a pressure head of 994 Pa. As compared to the other ferrofluidic micropumps, the best volumetric efficiency, pumped energy per cycle, and self-pumping frequency of the presented pump were higher than the other reported ferrofluidic micropumps.

Acknowledgement

The authors are grateful to Optics and Laser Laboratory at Sharif University of Technology for help with recording measurements.

References

[1] N.T. Nguyen, X. Huang, T.K. Chuan, MEMS-micropumps: a review, J. Fluids Eng. 124 (2) (Jun. 2002) 384–392.
[2] A. Nisar, N. Afzulpurkar, B. Mahaisavariya, A. Tuantranont, MEMS-based micropumps in drug delivery and biomedical applications, Sens. Actuators B: Chem. 130 (2) (2008) 917–942.
[3] D.J. Laser, J.G. Santiago, A review of micropumps, J. Micromech. Microeng. 14 (6) (2004) R35–R64.

[4] B.D. Iverson, S.V. Garimella, Recent advances in microscale pumping technologies: a review and evaluation, Microfluid. Nanofluid. 5 (2) (2008) 145–174.
[5] C-Y. Lee, Z-H. Chen, Valveless impedance micropump with integrated magnetic diaphragm, Biomed. Microdevices 12 (2) (2010) 197–205.
[6] J. Ni, B. Wang, S. Chang, Q. Lin, An integrated planar magnetic micropump, Microelectron. Eng. 117 (Apr. 2014) 35–40.
[7] C. Yamahata, F. Lacharme, Y. Burri, M.A.M. Gijs, A ball valve micropump in glass fabricated by powder blasting, Sens. Actuators B: Chem. 110 (1) (2005) 1–7.
[8] C. Yamahata, C. Lotto, E. Al-Assaf, M.A.M. Gijs, A PMMA valveless micropump using electromagnetic actuation, Microfluid. Nanofluid. 1 (3) (2005) 197–207.
[9] T. Pan, S.J. McDonald, E.M. Kai, B. Ziaie, A magnetically driven PDMS micropump with ball check-valves, J. Micromech. Microeng. 15 (5) (2005) 1021–1026.
[10] S. Haeberle, N. Schmitt, R. Zengerle, J. Ducree, Centrifugo-magnetic pump for gas-to-liquid sampling, Sens. Actuators A: Phys. 135 (1) (2007) 28–33.
[11] M. Shen, L. Dovat, M.A.M. Gijs, Magnetic active-valve micropump actuated by a rotating magnetic assembly, Sens. Actuators B: Chem. 154 (1) (2011) 52–58.
[12] N.T. Nguyen, Micro-magnetofluidics: interactions between magnetism and fluid flow on the microscale, Microfluid. Nanofluid. 4 (2012) 1–16.
[13] I. Torres-Díaz, C. Rinaldi, Recent progress in ferrofluids research: novel applications of magnetically controllable and tunable fluids, Soft Matter 10 (43) (2014) 8584–8602.
[14] B. Wagner, M. Kreutzer, W. Benecke, Permanent magnet micromotors on silicon substrates, J. Microelectromech. Syst. 2 (1) (1993) 23–29.
[15] N. Greivell, B. Hannaford, The design of a ferrofluid magnetic pipette, IEEE Trans. Biomed. Eng. 44 (3) (1997) 129–135.
[16] R. Pérez-Castillejos, J.A. Plaza, J. Esteve, P. Losantos, M.C. Acero, C. Cané, F. Serra-Mestres, The use of ferrofluids in micromechanics, Sens. Actuators A: Phys. 84 (1–2) (2000) 176–180.
[17] A. Hatch, A.E. Kamholz, G. Holman, P. Yager, K.F. Bohringer, A ferrofluidic magnetic micropump, J. Microelectromech. Syst. 10 (2) (2001) 215–221.
[18] E.G. Kim, J.G. Oh, B. Choi, A study on the development of a continuous peristaltic micropump using magnetic fluids, Sens. Actuators A: Phys. 128 (1) (2006) 43–51.
[19] N.T. Nguyen, M.F. Chai, A stepper micropump for ferrofluid driven microfluidic systems, Micro Nanosyst. 1 (1) (2009) 17–21.
[20] Y. Sun, Y.C. Kwok, N.T. Nguyen, A circular ferrofluid driven microchip for rapid polymerase chain reaction, Lab Chip 7 (8) (2007) 1012–1017.
[21] C. Yamahata, M. Chastellain, V.K. Parashar, A. Petri, H. Hofmann, M.A.M. Gijs, Plastic micropump with ferrofluidic actuation, J. Microelectromech. Syst. 14 (1) (2005) 96–102.
[22] H. Hartshorne, C.J. Backhouse, W.E. Lee, Ferrofluid-based microchip pump and valve, Sens. Actuators B: Chem. 99 (2–3) (2004) 592–600.
[23] B. Ando, A. Ascia, S. Baglio, A. Beninato, The One drop ferrofluidic pump with analog control, Sens. Actuators A: Phys. 156 (1) (2009) 251–256.
[24] B. Ando, A. Ascia, S. Baglio, N. Pitrone, Ferrofluidic pumps: a valuable implementation without moving parts, IEEE Trans. Instrum. Meas. 58 (9) (2009) 3232–3237.
[25] Ferrotec Corporation, USA, Technical data sheet, ferrofluid type: EFH1, Retrieved from: https://www.ferrotec.com/, Sep. 2010.

Biographies

M. Ashouri is pursuing the Ph.D. degree in the Department of Mechanical Engineering at Sharif University of Technology, Tehran, Iran. He received his B.S. and MSc degrees in 2007 and 2010, respectively from Sharif University of Technology. His graduate studies focus on micropumps and ferrohydrodynamic phenomena.

M.B. Shafii received the Ph.D. degree in mechanical engineering from Michigan State University, East Lansing, in 2005. He is currently an Associate Professor in the Mechanical Engineering Department, Sharif University of Technology, Tehran, Iran. His research interests include fluid diagnostic techniques (molecular tagging velocimetry, particle image velocimetry, and laser-induced fluorescence), heat transfer, phase change, micropumps, and heat pipes.

A. Moosavi received the Ph.D. degree in mechanical engineering from Lappeenranta University of Technology, Finland, in 2003. His research interests include micro- and nanoscale heat transfer and fluid flow. He is currently an Associate Professor in the Mechanical Engineering Department, Sharif University of Technology, Tehran, Iran.

H. Amiri Hezave received his B.S. and MSc degrees from Iran University of Science and Technology and Sharif University of Technology, respectively. His graduate studies focused on micropumps.